Interpretation of Enzyme Leach[SM] Survey Data from the Stope Baby Base and Precious Metals Prospect, Horsefly, B.C., Otish Mountain Exploration

by Gregory T. Hill
Consulting Geologist/Geochemist
30 September 2003

Interpretation of Enzyme Leach[SM] Survey Data from the Stope Baby Base and Precious Metals Prospect, Horsefly, B.C., Otish Mountain Exploration

by Gregory T. Hill
Consulting Geologist/Geochemist
30 September 2003

Summary

Three target areas have been defined within an Enzyme Leach[SM] survey conducted on the Stope Baby property. A complex geochemical distribution is present which includes significant metals responses including Au, Ag, Cu, Pb, Bi, and others. Oxidation anomaly patterns appear to be strongly structurally controlled suggesting the presence of several faults in the subsurface. Targets A and B are interpreted to represent reduced, metal-bearing zones that are peripheral to a possible syenitic intrusive body beneath target C. Drill testing of the three target areas is recommended. In addition, increased soil sampling is also recommended to better define the oxidation anomalies revealed through this survey.

Enzyme Leach[SM] Patterns

Enzyme Leach[SM] analysis of *B*-horizon soils reveals element patterns related to reduced bodies including mineral deposits in the subsurface. These patterns form in response to active electrochemical cells that are fueled by the subtle oxidation and/or bio-oxidation of buried reduced bodies (Clark, 1997). As a reduced body sheds electrons toward the surface, a reduced chimney is established vertically above that body. Volatile species involving oxidation suite elements are formed at the oxidation/reduction interface and these rise vertically along and outside the boundary of the reduced chimney. When the gasses reach the surface, a portion is trapped in amorphous oxide coatings on mineral grains, thus forming halo patterns around a central low. In addition, voltage gradients set up at the top of the reduced chimney (i.e. at the surface directly above the reduced body) cause the redistribution of some elements, already present at the surface, into halos and depletion zones. Some elements also form highs directly above reduced bodies or fault traces (Clark and Hill, 2000) . The term oxidation anomaly refers to the combination of these patterns.

Oxidation anomaly patterns tend to be characterized by oxidation halos which characteristically include at least part of the oxidation suite: Cl, Br, I, Mo, As, Sb, W, Re, V, Se, Te, U, Th. Where robust electrochemical cells are present, some or all of the metals, rare earth elements, lithophile elements, precious metals, and platinum group elements will also migrate into oxidation halos. Oxidation halos are typically asymmetrical, and may require comparison of a number of trace element patterns before they become apparent. Where a strong oxidation cell is present in the

subsurface, nested halos are often present, in which a single element forms ring-shaped or elliptical highs of differing dimensions positioned one within another (Hill and Clark, 2000). Elemental zoning in which different elements form halos of different dimensions is also typical in oxidation halos above mineral deposits. Recognizing nested halo patterns, zoning, and depletion can be of great assistance in vectoring toward the center of an anomaly. These features are also important in assessing the intensity of the system responsible for the formation of an oxidation anomaly. In order to detect nested halos and depletion zones, sample spacing must be sufficiently small, because the depletion zones and individual halos within a nested set can be quite narrow. A sample spacing of 25% or less of the width of the subsurface deposit is usually necessary.

Where more than one reduced body is present, oxidation anomalies are frequently combined or partially overlap. Under these circumstances, oxidation patterns related to reduced bodies tend to interfere with one another making recognition of anomalies above individual reduced bodies more difficult. Other difficulties stem from the fact that the oxidation anomalies commonly extend beyond the limits of the surveyed area. Sorting out these patterns requires a careful analysis of the data, a working model of the geochemical system, and experience. Where two or more deposits occur beneath the same soil survey, they will often have significantly different surface signatures. These differences can relate to variability in composition, depth, host rocks, size, or a number of other factors. The interpretation of these data rely on pattern recognition in conjunction with other available geologic and geophysical information. Thus, the interpretation of Enzyme Leach^{SM} data is enhanced by comparison with other available project data.

Design of Soil Survey, Sample Collection, and Analysis

B-horizon glacial drift soils were collected from 262 sites at 50 meter intervals along seven east-west sample traverses separated by 250 meters, except for the southernmost line which is separated by 300 meters (Figure 1). The sample distribution was designed by and sampling was carried out under the supervision of L. Goldsmith. According to Pezzot (2003) sample lines show a small amount of disparity from an ideal grid. Samples were plotted according to the local grid coordinates provided as a part of the sample identifications.

Prior to the involvement of Otish Mountain Exploration the author has visited the field area and is familiar with the geology and mineral deposits in the region. Samples were received at Actlabs in Ancaster, Ontario where they were analyzed by enhanced Enzyme Leach^{SM} in July 2003 and reported 13 August 2003. Data used in this interpretation are from Actlabs job number: A03-1541 (31541rpt.xls).

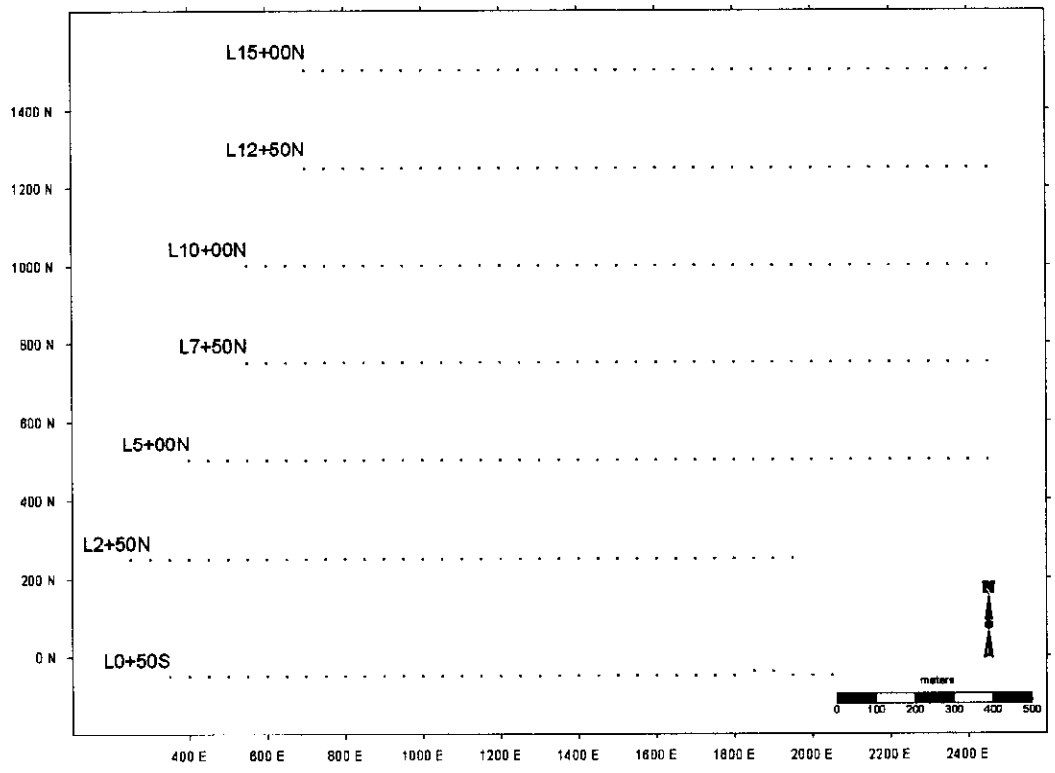

Figure 1. Sample locations

Data Treatment and Presentation

Surfer v. 7.0 and Excel v. 7.0 software were used to process and display the geochemical data. The plots utilize a color image map based on Kriged data using a 22 m. by 22 m. cell spacing. Linear distributions were used when making these maps because various transforming methods, such as log transforms, conceal important features in the data and because non-transformed data tend to yield plots with the most distinctive diagnostic geochemical patterns. It is important to recognize that different data treatments and plotting protocols can and often do have significant impacts on the resulting maps. Therefore, some elements are gridded and plotted in various ways throughout the interpretation process. The recognition of many of the patterns discussed here has benefitted from multiple views of the data.

Results and Discussion

A complex distribution of elements reveals several target areas within the surveyed area. The anomalies associated with the targets are superimposed on each other and there is considerable interference between anomalies. The subsurface structural fabric exerts strong controls on the distribution of trace elements as evidenced by the linear patterns (highs, lows, and gradients) developed in the distributions of individual elements. Several of the most prominent of these linear patterns are shown as interpreted faults along with target zones A, B, and C in Figure 2. Due to the sample distribution, north-south trending linears are quite recognizable but east-west oriented features are much more difficult to recognize. Therefore, east-west structural features have not been included in the summary map although there are suggestions that some may exist.

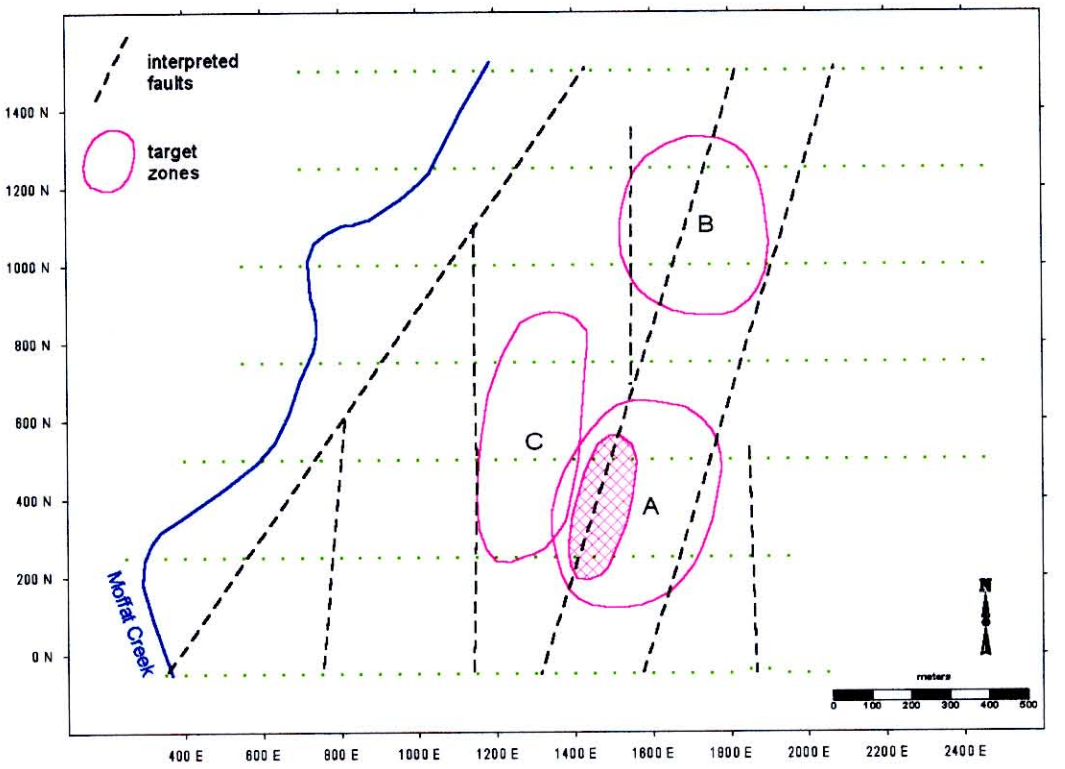

Figure 2. Interpreted faults and target zones A, B, and C.

Base and Precious Metals

Gold and Ag are enriched in a northwest trend in the northeastern half of the grid (Figure 3). This trend also contains strong Bi, In, and Hg responses (Figure 4). Although some of these metals are enriched in the same samples, there is significant zoning developed, with Bi and In present throughout whereas Au and Ag have more discrete distributions. Some important indications of underlaying structure are contained within the Au and Bi distributions. These elements indicate two parallel north-northeast trending faults that cut the subsurface beneath targets A and B. These interpretations of structures, as well as the others shown in the summary overlay, are consistent with the distributions of the other elements measured in this survey. These elements do not form halo patterns although they are discontinuously distributed into halos (defined by other elements) around targets A, B, and C, and an apical high within target A.

Copper is distributed into a distinctive halo around target A and also forms a broad high associated with Moffat Creek (Figure 5). Although mineralization beneath Moffat Creek cannot be ruled out, the Cu values around this stream appear to be reflecting a different sample media contained within the stream channel. Alternatively, the broad Cu high near Moffat Creek may represent a portion of an outer halo associated with the robust target A anomaly. Even if this is the case, Moffat Creek certainly influences the geochemistry as evidenced by increased background values in several other metals including Co, Ni, Cd, and most remarkably Tl (Figure 6). The area of increased Cu background in the western part of the survey approximately coincides with an area described as having conductive overburden (Pezzot, 2003).

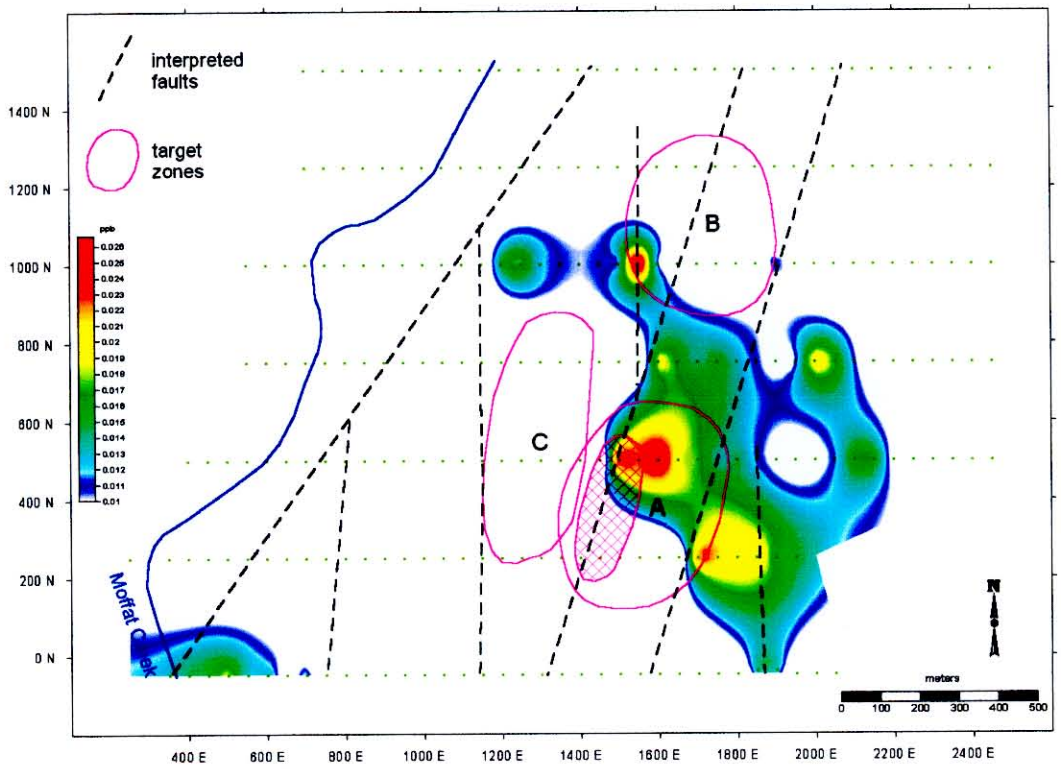

Figure 3. Gold distribution, interpreted faults, and target zones A, B, and C.

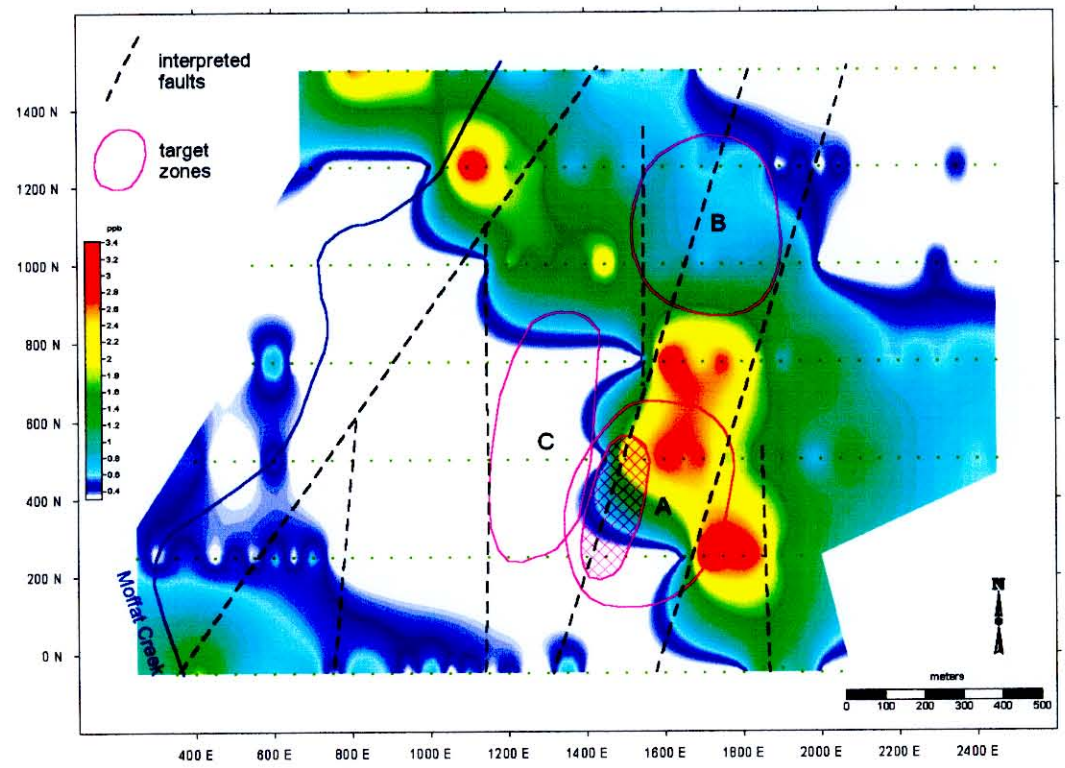

Figure 4. Bismuth distribution, interpreted faults, and target zones A, B, and C.

Thallium is contained in some sulfide minerals and also in feldpars where it substitutes for potassium. Because no lithophile elements show increased background values associated with Moffat Creek, and because of the correspondence of Tl, Cu, Co, Ni, and Cd enrichments, the preferred explanation is that the enrichments of these metals near Moffat Creek are derived from weathering sulfides within overburden. The presence of detrital sulfides within this stream channel would be capable of producing the observed patterns. In addition, Tl also forms more subtle but distinctive broad halos around targets A and B. Any Tl enrichments at the levels seen associated with targets A and B would be swamped out by the increased background associated with the Moffat Creek channel. The same is likely true of many other elements as well.

Lead forms linear patterns indicating that the Enzyme Leach[SM] responses of this metal are strongly controlled by north and north-northeast trending faults (Figure 7). These responses indicate an enrichment in Pb within the subsurface in the area that contains targets A, B, and C. This distribution also suggests that Pb may be dispersed into distal portions of mineral deposits in the subsurface.

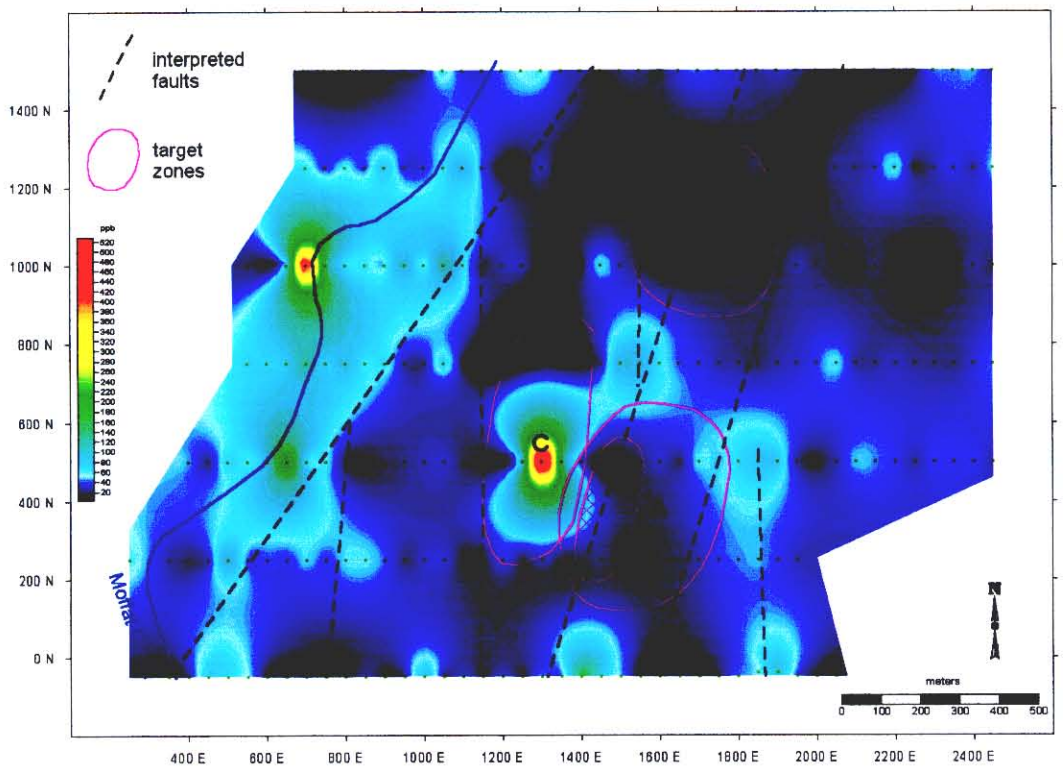

Figure 5. Copper distribution, interpreted faults, and target zones A, B, and C.

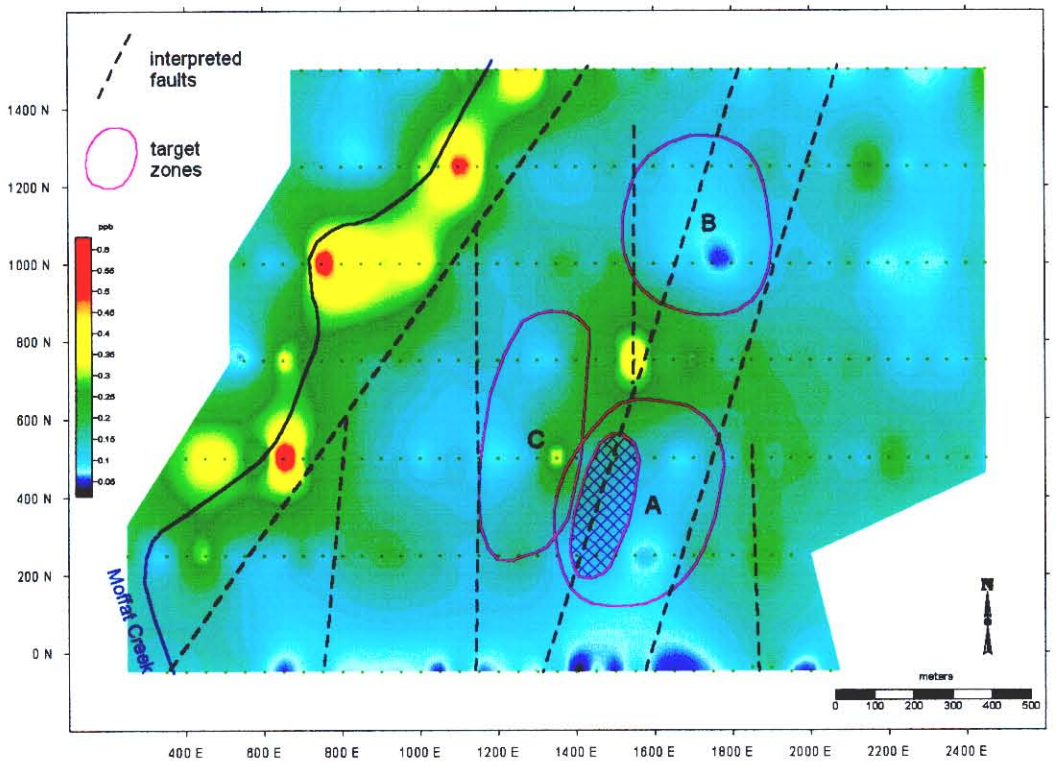

Figure 6. Thallium distribution, interpreted faults, and target zones A, B, and C.

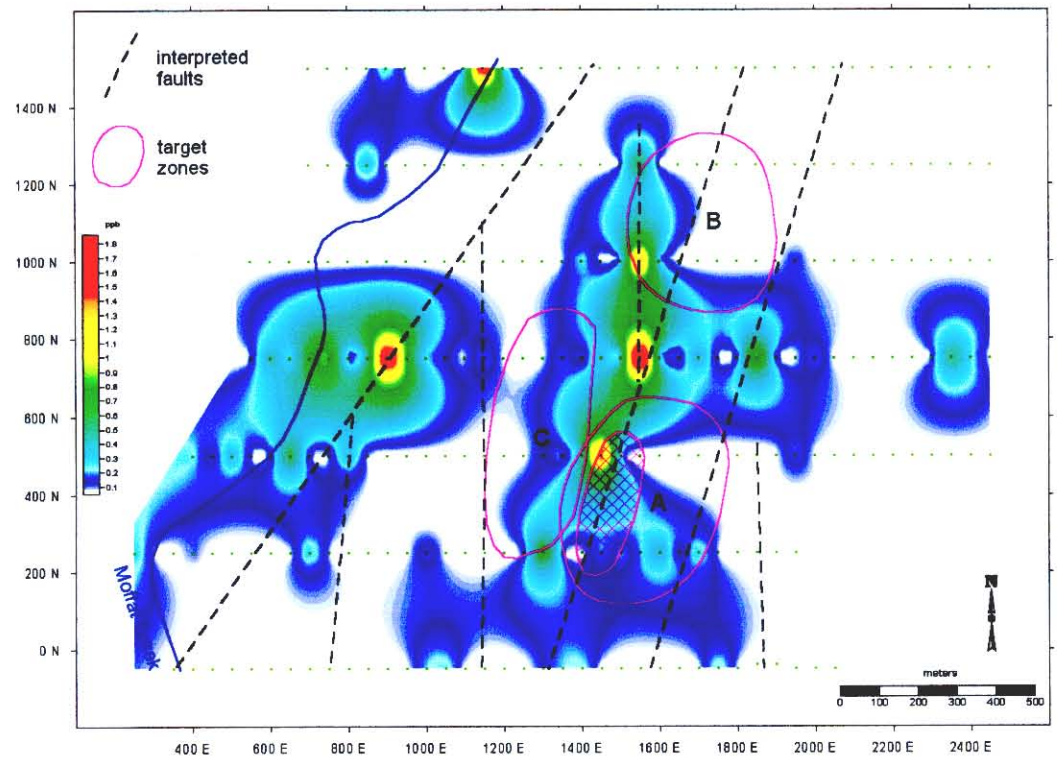

Figure 7. Lead distribution, interpreted faults, and target zones A, B, and C.

Oxidation Suite Elements

Most oxidation suite elements clearly show an oxidation halo associated with target A. Thorium shows one of the most distinctive halos (Figure 8). The halogens, Cl, Br, and I are also distributed into a distinctive halo around Target A. Normalizing these elements to their means and summing produces a distribution that shows the halo there (Figure 9). The patterns developed among most oxidation suite elements suggest that the target A anomaly may actually extend to the south-southeast of the sampled area as most are open in that direction.

Rhenium, Se, and W are distributed into halos around target A but do not form distinctive patterns that are diagnostic of the other target areas. Some elements, such as W form halos around relatively narrow central lows at target A (Figure 10). These narrow target A central lows are shown as a hachure pattern and are interpreted to represent a relatively sulfide-rich portion of an inferred mineralized system at depth. Arsenic, Sb, V, and U form halos around targets A and B but not target C.

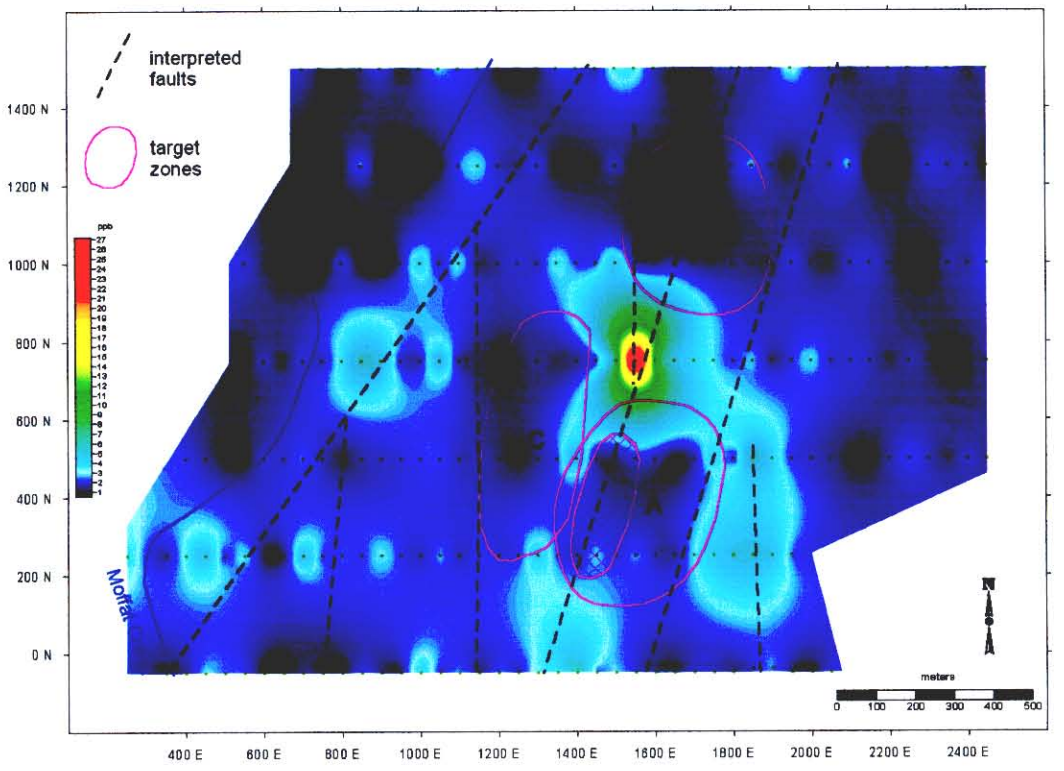

Figure 8. Thorium distribution, interpreted faults, and target zones A, B, and C.

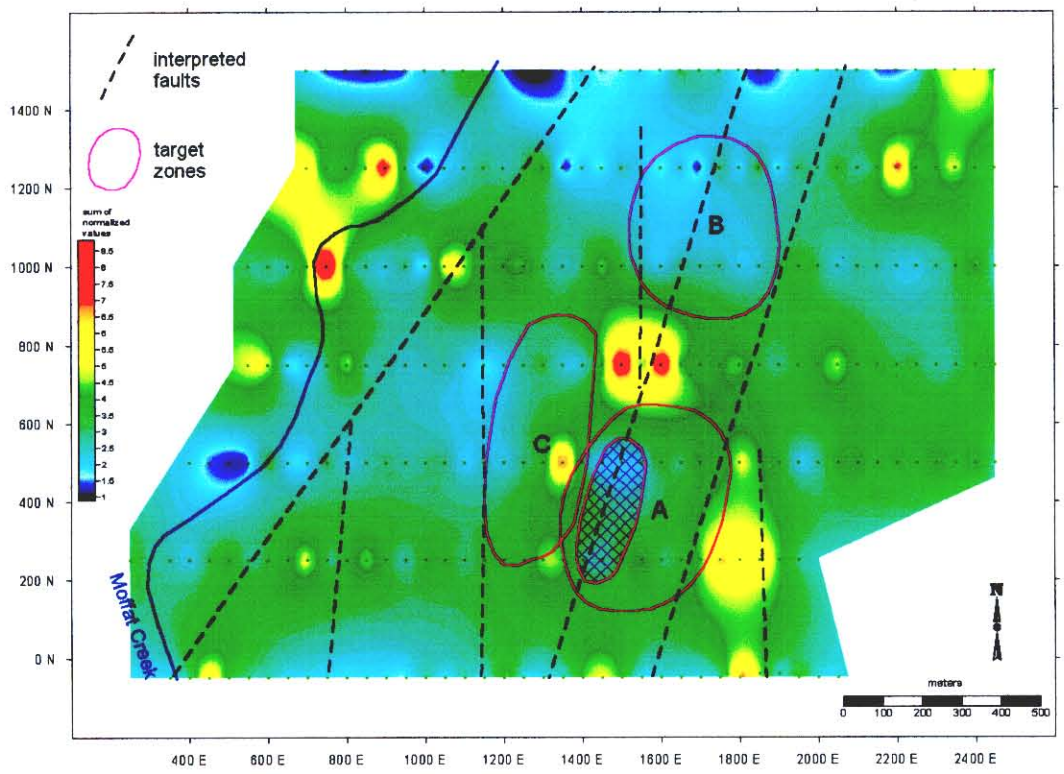

Figure 9. Sum of chlorine, bromine, and iodine normalized to means.

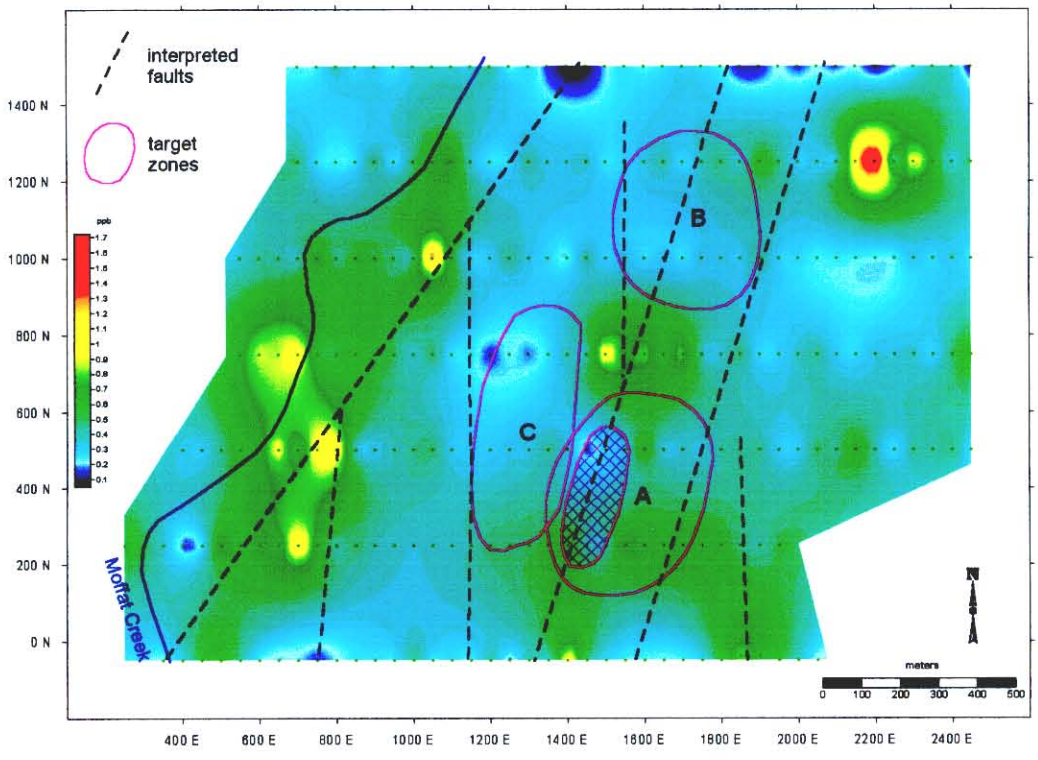

Figure 10. Tungsten distribution, interpreted faults, and target zones A, B, and C..

High Field Strength Elements

Zirconium and Hf form very subtle halos around target A and show little or no indication of targets B and C. The other HFSE, Nb, Ti, Y, and Cr show more diagnostic patterns. Two of the most interesting are Nb and Ti. Niobium is distributed into several highs near the center and south center of the grid (Figure 11). These highs partially surround targets A, B, and C but do not define clear halos. A series of Nb lows near the margins of the grid appear to represent an annular Nb low surrounding target C at the center. This pattern, along with those of some lithophile elements, described below, suggest that the electrochemical cell associated with target C is robust and affects the entire grid area. A similar annular low appears to be present among the Ti distribution (Figure 12). The highest values of this element are bounded between interpreted northeast trending faults on the east and west.

Rare Earth Elements

The REE form distinctive halos around targets A and B. A plot of Ce is shown as an example (Figure 13). The target A halos feature moderate enrichments of these elements. By contrast, the target B anomaly is characterized more by the presence of a depleted central low than by a distinctive halo. Compositional variation between the target A and B geochemical signatures is typical among the REE as well as many other elements and suggests that the subsurface beneath the two targets also varies significantly. One possibility is that a reduced body beneath target B is more deeply buried and/or more reduced/less oxidized than a reduced body beneath target A.

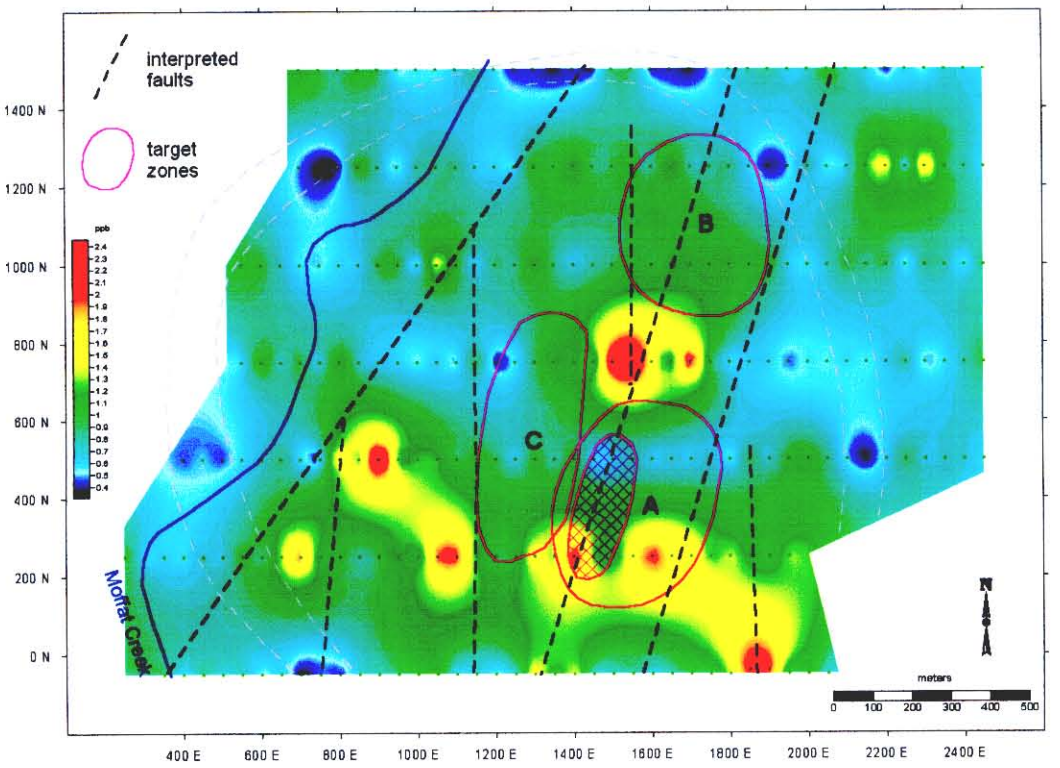

Figure 11. Niobium distribution with outline of annular low.

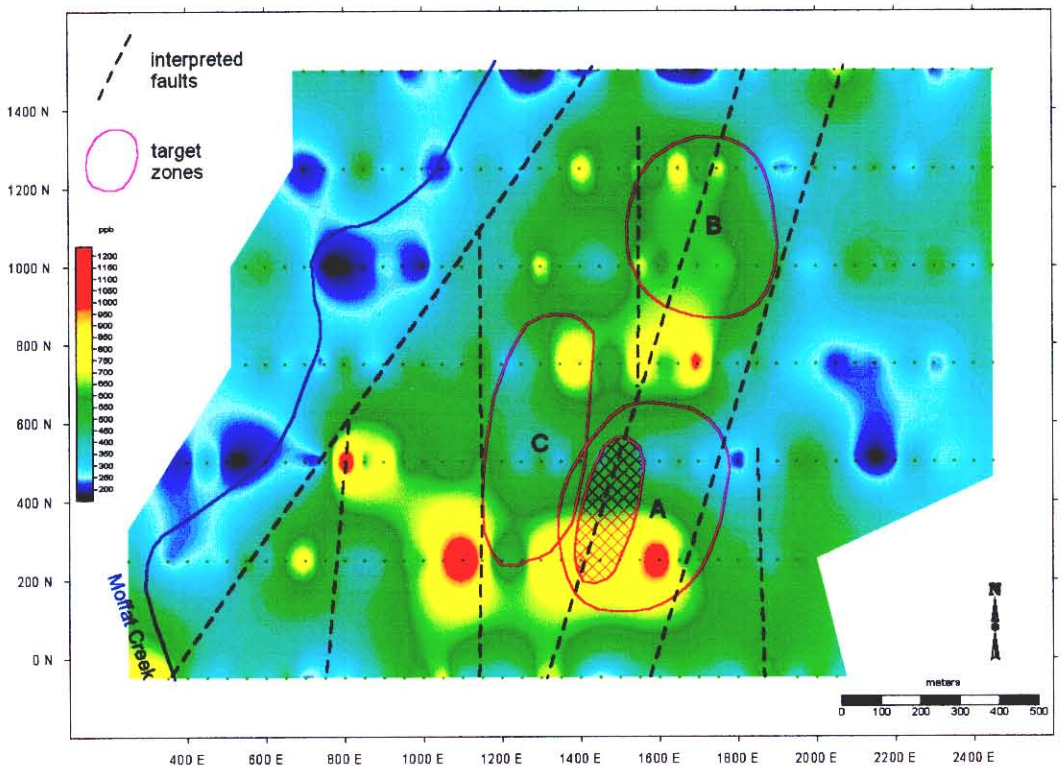

Figure 12. Titanium distribution, interpreted faults, and target zones A, B, and C.

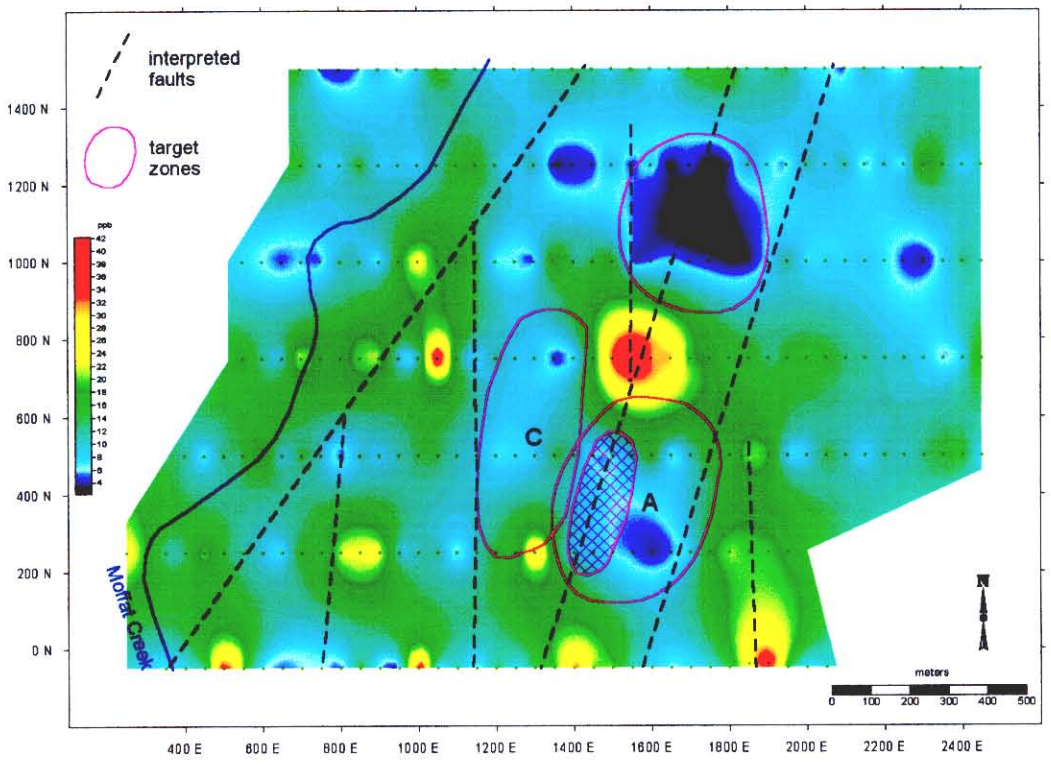

Figure 13. Cerium distribution, interpreted faults, and target zones A, B, and C.

Lithophile Elements

Beryllium and Ba form very distinctive halos around target C in the south center of the grid (Figures 14 and 15). These elements, along with some HFSE clearly define this target area. These lithophile elements are enriched in some intrusive rocks including syenite bodies and may therefore indicate the presence of syenite beneath target C. Furthermore, the strength of the Ba and Be halos along with the broad extent of the target C anomaly, as indicated by the Nb and Ti annular lows, suggests that an intrusive may be present beneath the target C area.

Conclusions and Recommendations

The complex patterns observed within the geochemical survey indicate the presence of at least three electrochemical cells, each of which interferes with the others. Although the most apparent target areas have been defined, there are indications that additional mineralized areas may also exist. For example, the broad northwest-trending Bi high and its attendant Au and Ag highs may indicate additional targets, particularly in the northwest. This enrichment could represent a northwest-trending fault zone with associated Bi-rich precious metals mineralization. The distributions of several elements, including Be, Ba, Nb, Ti, Cu, Tl, and others, indicate that the interpreted northeast trending fault zones shown on the figures bound the area containing targets A, B, and C, and offset the Au, Ag, Bi, In, and Hg trend. This suggests that the interpreted north-northeast faults have been active more recently than northwest-trending faults. The distributions of some other elements such as Ba also suggest that northwest trends are truncated against interpreted northeast-trending faults.

Additional sampling between sample lines would allow for a better understanding of these anomalies. An equant grid utilizing a 50 m by 50 m sample spacing would be ideal for this purpose. However, a more broadly spaced grid, such as 100 m by 50 m or even 100 m by 100 m would also be very useful in better resolving these anomalies and others that may exist but were not recognized at the current sample spacing.

Drilling is recommended to test targets A, B, and C with the highest priority being assigned to target A. At least two drill holes should be collared within each of the target areas. Because there is strong evidence of structural controls, angled holes designed to cut the interpreted structures where they intersect the target area outlines are recommended. The highest priority drilling should be focused on the northern and southern portions of target A. Targets B and C are assigned lesser priorities.

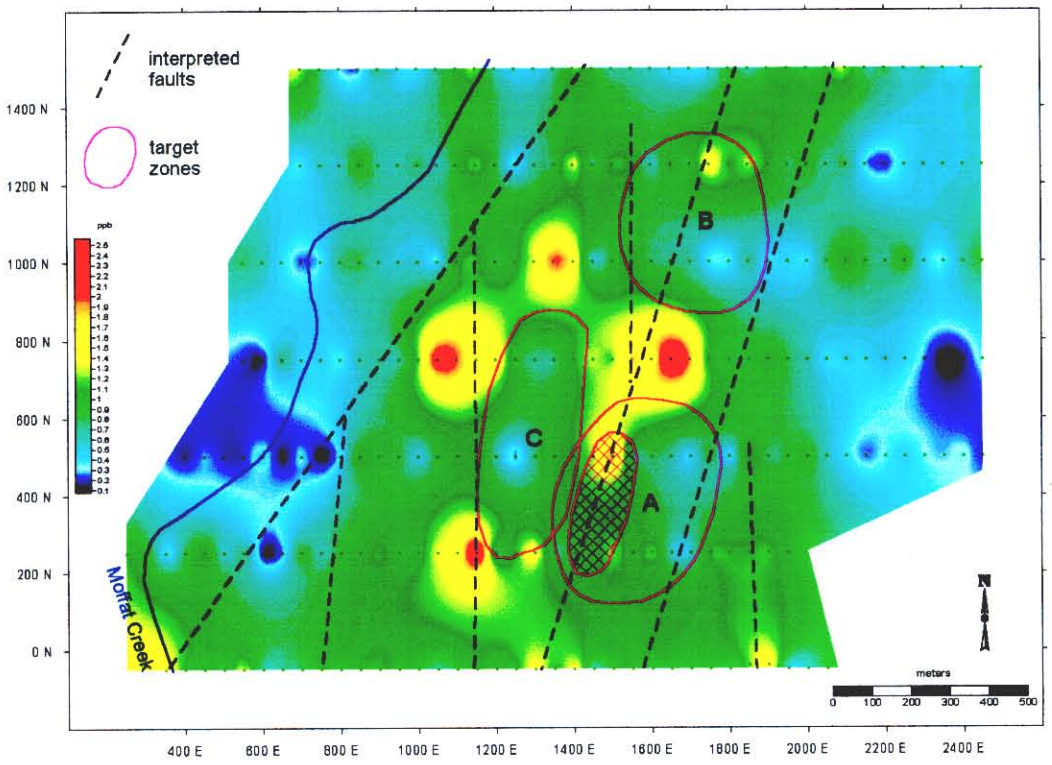

Figure 14. Beryllium distribution, interpreted faults, and target zones A, B, and C.

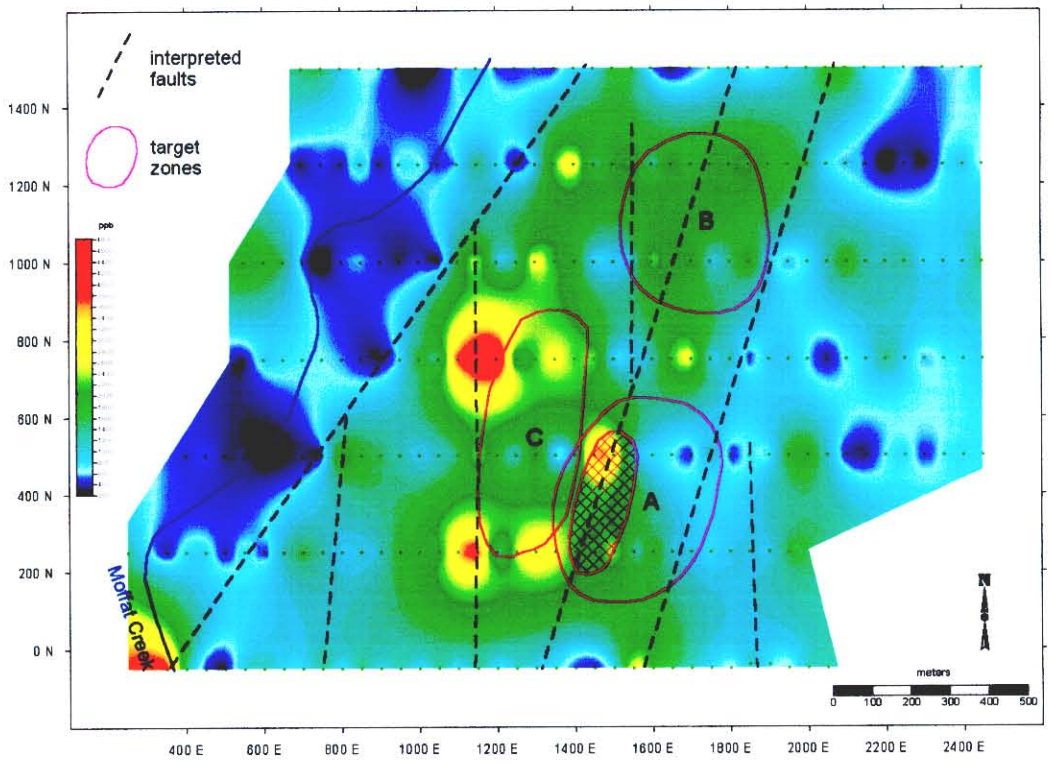

Figure 15. Barium distribution, interpreted faults, and target zones A, B, and C.

References

Clark, 1997, Enzyme Leach Model, Sampling, Protocol, and Case Histories, Actlabs Technical Manual.

Clark, J.R., and Hill, G.T., 2000, Structural Control of Oxidation Anomalies Above Buried Mineral Bodies, *in* Cluer, J.K., Price, J.G, Struhsacker, E.M., Hardyman, R.F., and Morris, C.L., eds., Geology and Ore Deposits 2000: The Great Basin and Beyond, Geological Society of Nevada Symposium Proceedings, Vol. II pp. 883-891.

Hill, G.T. and Clark, J.R., 2000, Enzyme Leach Signatures of the Marigold 8 North and Clay Pit Gold Deposits, Humboldt County, Nevada, *in* Cluer, J.K., Price, J.G, Struhsacker, E.M., Hardyman, R.F., and Morris, C.L., eds., Geology and Ore Deposits 2000: The Great Basin and Beyond, Geological Society of Nevada Symposium Proceedings, Vol. II pp. 903-918.

Pezzot, E.T., 2003, Logistics and Interpretation Report on Magnetic and Electromagnetic Surveys, Horsefly Project, S.J. Geophysics Ltd., Otish Mountain Exploration internal report, 14 pp..

Gregory T. Hill, M.Sc.
Consulting Geologist/Geochemist
785 Andrew Lane
Reno, NV 89521
775-849-2135

400 E 600 E 800 E 1000 E 1200 E 1400 E 1600 E 1800 E 2000 E 2200 E 2400 E

1400 N 1200 N 1000 N 800 N 600 N 400 N 200 N 0 N

interpreted faults

target zones

Nb annular low

B

C

A

Moffat Creek

N

meters

0 100 200 300 400 500

Scale 1:5000

Otish Mountain Exploration
Stope Baby Project
Enzyme Leach Survey

Anomaly Summary Map

Drawn by: G.T. Hill Date: 30 Sept 2003

Data Source: A03-1541 (31541rpt.xls)

27258 3/3
(M1)